Design and Experimental Validation of a Process Chain for Thin Components Manufacturing by Micro Injection Molding Process

Design and experimental validation of a process chain for thin components manufacturing by micro injection molding process

Bellantone, Lavecchia, Surace, Spadavecchia, Modica, Guerra, Fassi, Galantucci

Micro applications, especially in biomedical and optical sectors, require the fabrication of thin polymeric parts which can be commonly realized by micro injection molding process. However, this process is characterized by a relevant constraint regarding the tooling. Indeed, the design and manufacturing of molds could be a very time-consuming step and so, a significant limitation for the rapid development of new products. Moreover, if the design displays challenging micro-features, their realization could involve the use of more than one mold for the fabrication of a single thin part. Therefore, a proper integration of different manufacturing micro technologies may represent an advantageous method to realise such polymeric thin micro features. In this work, a micro-manufacturing process chain including stereolithography, micro milling and micro injection molding is reported. The mold for the micro injection molding process was fabricated by means of stereolithography and micro milling, which allowed to produce low-cost reconfigurable modular mold, composed by an insert support and a removable insert. The assessment of the proposed process chain was carried out by evaluating the dimensions and the surface finishing and texturing of the milled mold cavities and molded components. Finally, a brief economic analysis compares three process chains for fabricating the micro mold showing that proposed one reduces manufacturing cost of almost 70% with the same production time.

1. Introduction

In the last years, the miniaturization of high precision components has become a fundamental element of modern industry bringing the development of micro and nano technologies that comprise micro Electro Discharge Machining (EDM), micro traditional machining (milling, cutting), laser cutting/patterning/drilling, micro extrusion, micro embossing, micro stamping, micro injection molding. The growing demand for micro components involves many sectors including aerospace, automotive, electronics, telecommunications and in particular biomedical and optical sectors for specific applications of thin components [1]. Consequently, a proper integration of different manufacturing micro technologies may represent an advantageous method to realise such thin micro features.

In this context, micro injection molding is a key enabling technology due to its advantages as simple forming process, high production rate, low cost, stable product quality and it has been applied for

forming many products, especially polymeric, as sensors, actuators, microfluidic devices and optical lens. At microscale, the cavity filling is a challenging task in particular for thin parts with dimension of around 100 µm that experience very fast cooling and solidification during injection, resulting in a short travelling distance of melt flow [2]. In fact, in thin and large plastic plate with thickness of 300 µm or less, the molding is not easy due to the reduction in the fluidity of molten polymer by the solidified skin layer [3]. Underlined these issues, it is also essential to control, accurately, the parameters that are of critically importance for the replication quality of micro parts and, therefore, they have been extensively studied by many researchers [4–6]. The results indicate that the main process parameters that can affect the part quality include: melt and mold temperature, injection speed, holding time and pressure, but the literature findings about their influence are quite different depending from part geometry, polymer type and its properties, machine and finally from mold design and manufacturing. The direct relationship between parts quality and mold manufacturing method is very crucial and has been extensively demonstrated [7,8]. To accomplish this task, different advanced micro manufacturing techniques can be used [9,10] as micro cutting/milling [11], electroforming and laser-based processes [12], lithography techniques, micro EDM [4], additive manufacturing both for metallic [13] and polymeric molds [14].

Furthermore, new generation of hybrid technologies for tooling were established to overcome the bottlenecks of a single process in terms of obtainable features, removal rate, accuracy, surface finishing and the tools are manufactured with combination of micromachining techniques [15,16]. Concerning molds manufacture, two new challenges for reducing time and costs could be: firstly, the design of interchangeable modular mold and secondly the creation of molds integrating pieces made with different manufacturing technologies. About the first issue, the cavities can be produced on an insert which is then fitted in the main body of the mold that reduces the cost of process set-up and the time required for tooling. The second issue is the focus of the present paper. Since the mold is usually made of steel, insert can be manufactured also of other materials, for example polymers, depending on the used technology [10]. Here, two processes (stereolithography and micro milling) were applied for the realization of mold and insert, respectively, for polymeric thin parts manufacturing useful in microfluidics and optical applications.

Stereolithography (SLA) is a well-known additive manufacturing (AM) technology; it is a light-based process that builds individual layers of a model with liquid polymer, hardened by a laser beam. SLA is capable to print polymeric parts with high dimensional accuracy, smooth surface finishing and high features resolution with good mechanical properties. These features make this technology particularly suitable for small parts fabrication with challenging 3D shapes and geometry. SLA technology offers several advantages with respect to traditional manufacturing for molds and inserts fabrication because

it better fits the compromise between accuracy, cost and easy-to-use. The main drawbacks of the "soft" materials, used in AM processes for mold, are the thermal and mechanical properties and the toughness significantly different from steel. These properties negatively affect the tool durability at high temperature and the quality of the final products [17].

Micro milling is a downscaling of the conventional milling process, involving the use of endmills with diameters in the submillimetre range. This downscaling leads to a series of size effects, which negatively affect the process. Firstly, the grains size of material affects the finish of the worked surface; it is due to the small size of the chip which shouldn't be smaller than the grain size. Indeed, an investigation [18] has shown how the use of materials with small grain size and high homogeneity improves the surface finish of micro milled parts. The second effect is related to the cutting-edge radius. Indeed, when depth of cut is less than the minimum chip thickness, the cutting angle becomes negative and the effects of elastic return of the material and the ploughing action prevail with the consequence that the material is only deformed without any chip formation [1,19]. Another issue, due to the small size of process, is the runout, that is the eccentric deviation of the tool rotation axis from the theoretical one. Runout causes the deviation of the cutting-edge trajectory and, therefore, the variability of the uncut chip thickness removed by the different cutting edges generating vibrations, roughness worsening and accelerating tool wear [20].

Regarding the influence of process parameters on the machined surface finish, it is observed by Yuan et al. [21] that the surface roughness increases when increasing the feed per tooth and that the effect of the minimum chip thickness and runout decreases when the feed rate approaches the macro level. The experiments of Jing et al. [22] show that when the feed rate is lower than minimum uncut chip thickness, ploughing and elastic recovery occurred in micro milling rather than cutting action, and Ra decreases with the increasing of the feed rate. On the other hand, the shearing effect becomes dominant when cutting at high feed per tooth values. Regarding the cutting speed, the research of Zhang et al. [23] and Sun et al. [24] shows that increasing the spindle speed produces lower roughness values, although, at certain values of the spindle speed, tool vibrations occur, worsening the surface finish. Moreover, a tool with a smaller diameter is more subject to deformations therefore an increase of this one causes a decrease of roughness [22,25].

One of the more interesting applications of micro milling is the fabrication of micro molds, due to the suitable surface finish characteristics. In this context, Sodemann et al. [26] realized an aluminium mold to cast polymer-based microchannel devices assaying blood clot formation under varying shear rates, obtaining an average of Ra values of 0.15 μm. Vazquez et al. [27] realized an aluminium 7075 T6 mold for ultrasonic molding of a miniature classical guitar with an average of Ra values of 1.15 μm. With the aim to optimize the fabrication of micro milled mold inserts for hot

embossing microfluidic device, Chen et al. [28] realized a series of reservoirs on a brass substrate with Ra between 0.03-0.13 µm. Davoudinejad et al. [29] realized a hardened tool steel functional surface for injection molding composed of micro ridges with an average surface roughness (Sa) of 0.05 µm. Controlling the surface roughness is of great importance since the last directly affect the mold performance during the injection process [30,31].

In this work, a micro manufacturing process chain is reported including stereolithography, micro milling and micro injection molding for thin parts manufacturing. The mold was fabricated by means of stereolithography and micro milling which allowed to produce a modular double insert (composed by a support and a removable insert) to be assembled into the main mold. The micro injection mold was manufactured using stereolithography technology, while the interchangeable insert using micro-milling process. To demonstrate the effectiveness of this approach, a thin test part was designed, fabricated, and successfully tested. Furthermore, the cavities surfaces were produced with different roughness and texturing obtained by different milling strategies and, after a morphological surface characterization, their effect on the melt flow was studied through the analysis of the part filling. Finally, the production time and cost of the micro mold were estimated and compared for three different process chains. The objective of this economic analysis is to highlight the advantages of the implemented process chain aiming at decreasing time and cost for injection molding tooling.

2. Mold design and manufacturing

In micro injection process, the mold has to fullfill three functions: shape the part, sustain the pressure without distortion, and act as a heat exchanger to provide and remove heat from the molten plastic. Concerning with these factors, a carefully mold design is a critical task specially to achieve a high level of dimensional stability in the finished part. In this work, the mold has been realised in modular way and it is composed of three parts: a support realised by stereolithography that could be re-used, a disk (insert) with micro-milled thin cavities and the main plates on which the two parts were assembled (Fig.4). This combined approach allows to accomplish high accuracy and easily interchangeable geometry in acceptable machining times.

2.1. Design

The mold geometry consists of four crossed symmetrical wings. Each wing is 6 mm length, 3 mm width and 120 µm thick with a flat base and a draft angle of 2° (Fig. 1). The draft angle favours part demolding realised by an ejector pin moving through a central hole. The chosen design is a good target for both milling but specially molding because it is not easy to inject a thin and large plate due to the rapid solidification occurring at wall/part interface.

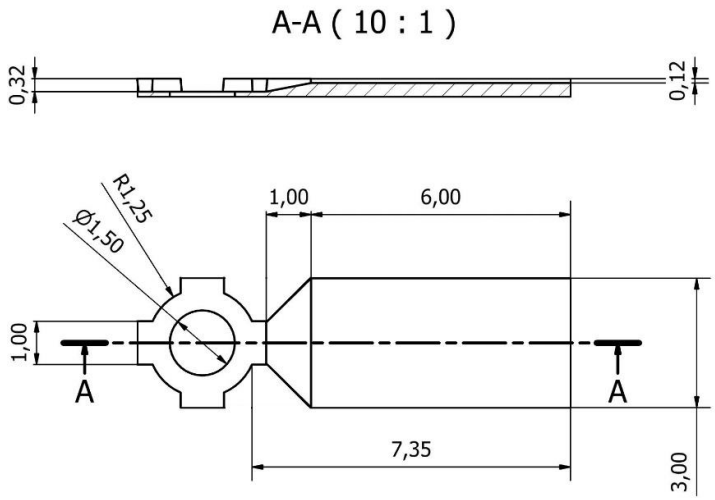

Fig. 1 Design of a single wing

2.2. Milling

For the micromilling process of the mold, a continuous 5-axes movement Kugler MICROGANTRY Micro machine was used, with accuracy on z axis of +/- 0.5 μm and maximum spindle rotation speed of 60000 rpm. During processing, the used coolant is a vaporized Vaseline oil. The mold material is a tool steel 1.2767 - Ni - Cr - Mo (DIN 17350) with hardness of 250 HV1. The metallographic analysis of this material revealed a microstructure with a grain size between 2 and 20 μm. The disk, on which the cavities will be machined, and the workpiece holder were assembled, and then were grinded on the top and bottom faces to ensure the planarity and parallelism of the two surfaces. The NC code of the micro milling process was generated using the commercial software Autodesk FeatureCAM from the CAD model of the tool (Fig. 2).

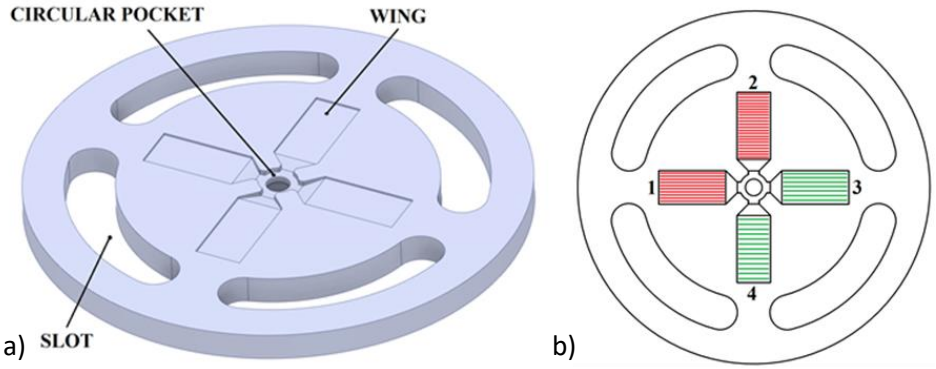

Fig. 2 a) CAD model of the disk and b) adopted milling strategies and wings number notation

The milling strategies adopted for the realization of the tool was divided in two main steps: roughing and finishing operations. In particular, the roughing was performed by an 800 μm diameter endmill using a spiral strategy, while the finishing operation was carried out by a 500 μm diameter endmill

using a parallel strategy. The choice of this strategy for the finishing operation is to create different topographies and consequently different flow conditions for the injected material, varying the machining direction for each wing. Figure 2b represents the finishing strategies adopted for the four wings, that differ for the feed rate and overlap, to obtain a better surface quality on the wings 1-2 (red) than 3-4 (green). Furthermore, in order to achieve the desired slope in lateral surface of the wings, a small depth of cut (4 μm) was used during the roughing phase, to minimize the stairs effect on the side walls. Finally, four circular slots were milled on the disk to facilitate its subsequent diameter reduction necessary for assembling in the resin support for micro injection process. The cutting parameters, shown in Table 1, have been selected considering the tool diameter and the desired roughness values on the bottom of the part. Fig. 3 shows the part after the micromilling process and before the micro milled plate cutting, to be assembled to the resin support.

Table 1 Milling process parameters

	Operation	Strategy	Tool diameter [μm]	Teeth number	a_z [μm/tooth]	Overlap [%]	p [μm]	n [RPM]	Feed rate Va [mm/min]
Circular Pocket	Roughing	Spiral	800	3	8	-	20	20000	475
Wing 1	Roughing	Spiral	800	3	8	50	2	20000	475
	Finishing	Parallel	500	3	2.3	70	4	40000	275
Wing 2	Roughing	Spiral	800	3	8	50	2	20000	475
	Finishing	Parallel	500	3	4.63	70	4	40000	275
Wing 3	Roughing	Spiral	800	3	8	50	2	20000	475
	Finishing	Parallel	500	3	2.3	10	4	40000	555
Wing 4	Roughing	Spiral	800	3	8	50	2	20000	475
	Finishing	Parallel	500	3	4.63	10	4	40000	555
Slots	Roughing	Spiral	3000	3	10	-	20	7300	220

a)  b) 

Fig. 3 a) Disk and workpiece holder after processing and b) particular of the machined cavities

2.3. Support printing and mold assembly

The resin support (Fig. 4a) was realised by stereolithography (SLA) using a Formlabs Form3 machine which implements a bottom-up exposure (inverted) stereolithography [32] with a 250 mW laser. It allows to accomplish a minimum feature size of 85 μm (laser spot diameter) with a positioning resolution of 25 μm on the XY plane and layer height from 25 to 300 μm. The support has been fabricated using a proprietary photo-sensible resin (Formlabs Grey resin V04), a standard resin having tensile strength comparable to ABS. The layer thickness has been set to 50 μm, in order to achieve part accuracy and reduced working time. After the part has been printed, it was washed in isopropyl alcohol for 20 minutes and it was ready for use after drying and support cutting. Two threaded holes have been created to lock the insert on the support with screws and a small central hole necessary for the part ejection (Fig. 4b). Then, the disk and support (Fig. 4c) were mounted on the main plate on injection machine after checking the planarity of assembled system (Fig. 4d).

Usually, when additive manufacturing is used for polymeric tool production, the major problems are the temperature of molten material and the stress that the mold must withstand both influencing strongly the tool life [33]. Instead, in the proposed solution, these drawbacks are partially overcome by the combination of the support realized by Additive Manufacturing technology and an insert made by steel realized using micro milling.

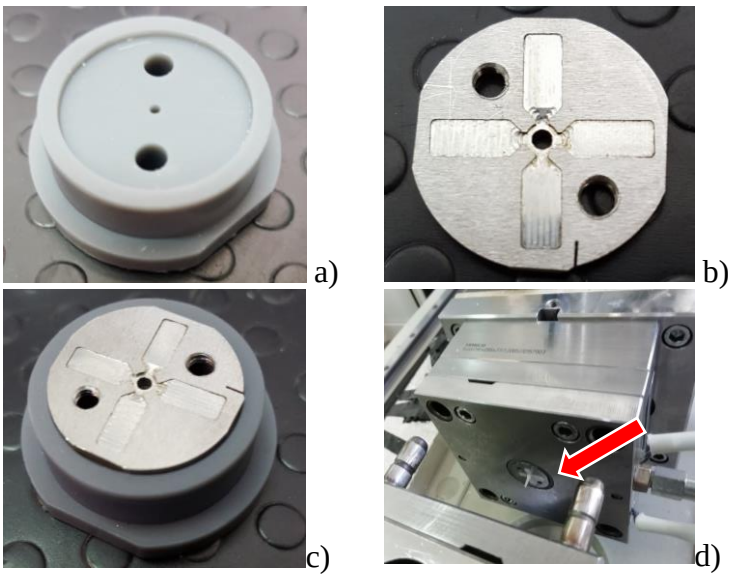

Fig. 4 a) Resin support, b) milled tool, c) assembled removable mold, and d) entire mold with main plate mounted on machine (with injected part before ejection)

3. Part manufacturing by micro injection molding

The micro molding machine used in injection experiments is the DesmaTec FormicaPlast 1K. This machine has a pneumatic injection drive and its architecture includes two plungers: a 6 mm diameter

piston for the pre-plasticization and a 3 mm diameter piston for the two-phase accurate injection. The maximum injection pressure, injection volume and injection speed of the machine are 300 MPa, 150 mm^3 and 500 mm/s respectively.

BASF's semi-crystalline Polyoxymethylene (POM) was selected to be injected as polymeric material for its characteristic: high toughness, hardness, stiffness, and good electrical behaviour. Its properties are reported in Table 2. Before use, POM was dried at 110 °C for 3 h to avoid water entrapment. The experimentation has been divided into two steps comprising the screening phase, in which different configurations of process parameters are tested for obtaining a complete part without defects, and a successively refined experimentation.

Initially, injection tests were carried out by setting mold and melt polymer temperatures at 80 °C and 230 °C respectively, as suggested from material's manufacturer and from previous experimentation [31]. The injection speed was set at 160 mm/s and the holding pressure and time at relatively low values due to the thin geometry of the part and to avoid flash formation (100 bar and 1 s). The cooling time was fixed at 5 s. From preliminary tests, appears clearly the difficulty to completely fill the mold, due probably to the high aspect ratio of the thin geometry causing the rapid freezing of the melt flow. Then, in order to improve the cavities filling, the injection speed has been increased favouring, thus, the filling but also increasing flash formation especially near the gate. The tests showing the best result were carried out setting the following process parameters: mold temperature 90 °C, melt temperature 240 °C, injection speed 170 mm/s while all the others were kept constant. Fig. 5 shows some molded samples obtained at varying injection speed.

Table 2. Material properties

Name	Trade name	Grade	Melt temperature	MVR (ISO 1133)	Density (ISO 1133)	Tensile modulus (ISO 527)
POM	Ultraform BASF	N2320 003	230 °C	7.5 cm^3/10min	1400 kg/m^3	2700 MPa

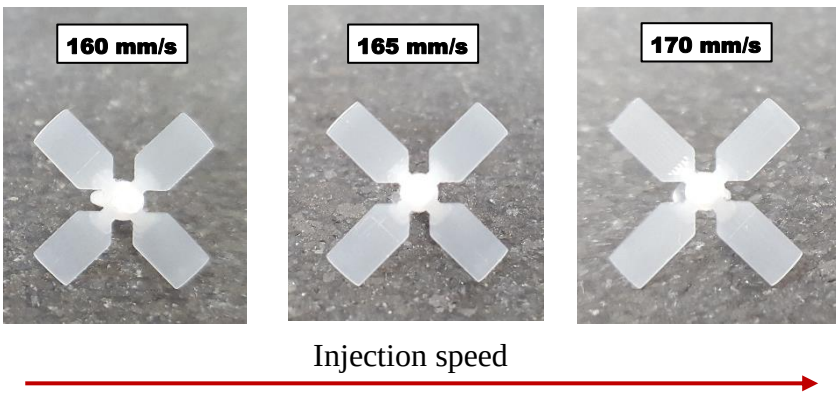

Fig. 5 Molded samples at increasing injection speed

4. Results and discussion

Hirox RH-2000 digital microscope was used to observe the micro-milled wings and the injected components. Taylor Hobson CCI MP-HS interferometer was used to perform dimensional and surface roughness measurements. All scans were carried out using a 20x lens, with a resolution of 1.0 μm on x-y plane and 0.01 nm on z axis and were analysed using Talymap Platinum software according with the standard for measurements with non-contact instruments (ISO 25178). For the analysis of the side walls of the thin cavities, the technique of conoscopic holography was adopted using an Optimet ConoScan 4000 with a 25 HD lens with accuracy <1 μm and repeatability <0.2 μm.

4.1 Wings dimensional analysis

The measured dimensions (width and length) of milled wings differ slightly from the nominal ones as showed in Table 3. The deviations can be originated from different causes as the tool runout firstly and also by the difficultly acquisition for the identification of the wing upper edge due to the side wall inclination. From the image of wing 3 (Fig. 6) this inclination is not clearly visible nor quantifiable and it should correspond to the black border. Even from the conoscopic analysis, this inclination is difficult to identify (Fig. 7).

Table 3 Wings measured dimensions.

Wing	Width (μm)	Length (μm)	Depth (μm)
1	2984.36	6997.97	123
2	2997.37	6994.87	123
3	2984.40	6952.03	121
4	2994.39	6979.03	126

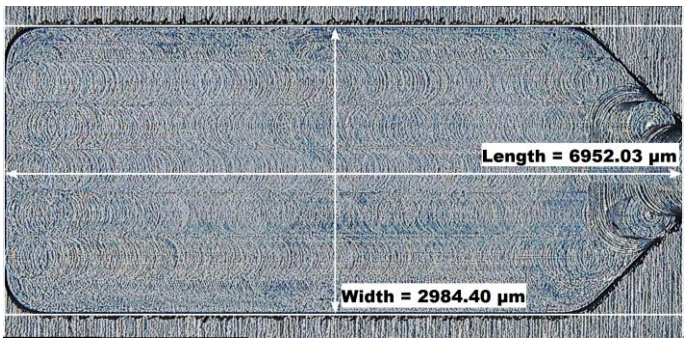

Fig. 6 Wing 3 image and measurements acquired by microscope

Fig. 7 Scanned images with conoscopic holography

4.2 Wings roughness evaluation

A three-points levelling of the analysed wings surface was performed using the profilometer software Talymap Platinum. For the surface roughness measurement, the following procedure was implemented: for each wing, five equidistant profiles along the flow direction (red lines Fig. 8) and six along the perpendicular direction (orange lines Fig. 8) have been extracted. Then, for each profile, the form removal was applied and the roughness was evaluated (Table 4) regarding the profiles orthogonal and parallel to the flow direction. The roughness values measured on the wings 3 and 4 orthogonally to the feed direction are higher than the ones measured on wings 1 and 2 due to the use of a higher feed rate and a different overlap. Surface roughness (Sa) was evaluated too and reported in Table 4.

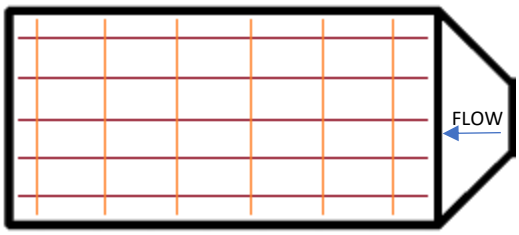

Fig. 8 Acquired roughness profiles on each wing

Table 4 Wings roughness evaluation

	Wing 1	Wing 2	Wing 3	Wing 4
Ra of orthogonal profiles to the flow direction (µm)	0.17	0.15	1.12	0.24
	0.10	0.11	0.45	0.14
	0.07	0.12	0.11	0.12
	0.09	0.10	0.09	0.10
	0.07	0.10	0.10	0.16
	0.11	0.09	0.51	0.08
Ra Mean value (µm)	0.10	0.11	0.40	0.14
Ra of parallel profiles to the flow direction (µm)	0.10	0.16	0.08	0.87
	0.06	0.11	0.05	0.29
	0.08	0.11	0.13	0.16

	0.10	0.13	0.10	0.59
	0.11	0.14	0.13	1.05
Ra Mean value (µm)	0.09	0.13	0.10	0.59
Sa (µm)	0.13	0.13	0.20	0.85

4.3 Molded components dimensional analysis

After dividing each sample in the four parts (1-2-3-4) corresponding to the four wings, the replication accuracy of the injection process was carried out by metrological characterization; microscope images were used for width and length measurements (example of part in Fig. 9) and a digital micrometre for thickness and then the obtained values were compared with tool dimensions.

Figure 10 reports the dimensional results for length (a) and width (b) of component (red dots) and mold (blue dots). As evident, the sample is not completely filled and the length is about the 82% of mold nominal values with a curved profile at the final edge (Fig.10a). This result is due to the high aspect ratio of the parts: the thickness of the wing is 1/60 of its length and, once the polymeric flow enters in the micro cavity, it rapidly freezes due to the quick heat transfer and thus, solidification occurs hindering the complete component filling. The cavity 3 is slightly better filled than the others, maybe because its surface shows high roughness and feed milling direction is parallel to the flow direction. Both of these conditions, but in particular the latter, have been previously found that can facilitate the thin cavities filling [31]. Differently, components width comparison (Fig. 10b) shows high correspondence between parts and mold and the difference is less than 2 µm, with no significant variation among the four values.

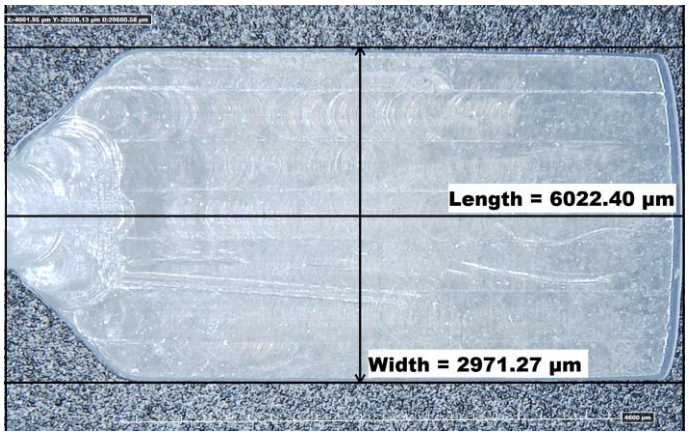

Fig. 9 Component image acquired by microscope

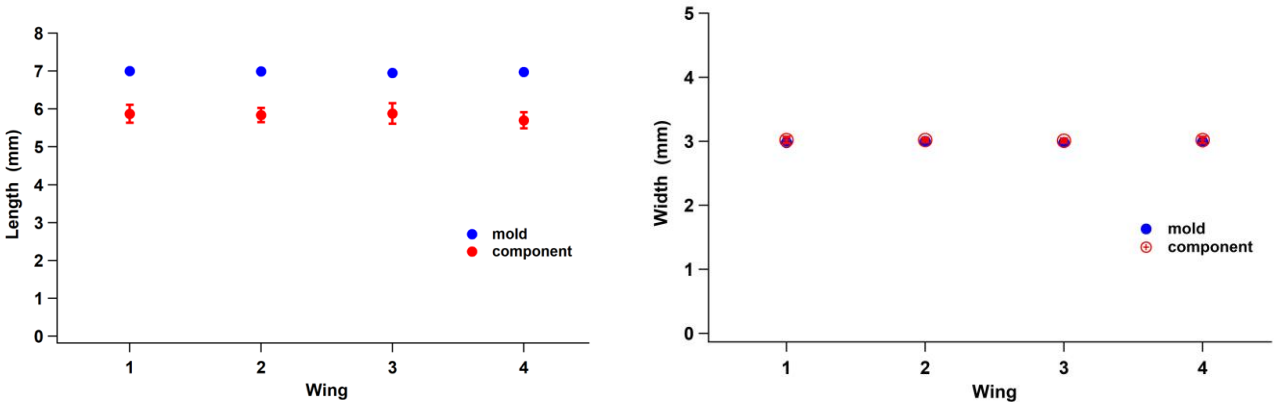

Fig. 10 Length (a) and width (b) results of the wings (blue) and components (red)

The analysis of surfaces by interferometer was carried out by positioning the parts on a Johansson gauge for performing a three-points levelling of the acquired scan and having a reference surface to calculate the height of the sample. From the colour distribution of the scans (Fig. 11), the non-uniformity of the filling appears evident. In fact, there is a decrement of the thickness from the gate towards the end of the part. However, an absolute thickness value of the parts could not be evaluated due to non-planarity of the surfaces; hence digital micrometre measurements were performed. Figure 11b reports parts thickness results measured in the middle of the sample. Molded parts are thicker than expected. A hypothesis explaining this result could reside in the mechanical properties of the resin support that could show a different behaviour during the injection process in comparison to a total steel mold. In fact, Young's modulus of the SLA resin is two order of magnitude lower than steel one, 2.8 GPa and 200 GPa respectively, as results from the corresponding material datasheets. During the filling phase of the process, the melt pressure in the cavity on the milled tool compress the resin support too that could have a different behaviour in comparison to a steel one. To verify this hypothesis, assembled mold was modelled in FE COMSOL Multiphysics® software as shown in Figure 12a. The overall mesh has 76696 tetrahedral elements with different dimensions and densities according to the two different domain geometries, for the milled disk and the resin support, respectively. The solid mechanics module has been used with a fixed constraint on the lower base of the model and a boundary load applied on the milled mold surfaces (wings and gates). Pressure value has been set at 230 bar, according to injection molding machine log file and a stationary study has been performed. Figure 12b shows the displacement magnitude in z direction of the cavity surfaces and the calculated displacement varies between 15 µm and 25 µm with an average value of about 20 µm which is consistent with the experimental ones. The simulation and experimental results suggest that the mechanical properties of the support material influence the injection process results and should be carefully considered in tool design. A further investigation will be carried out.

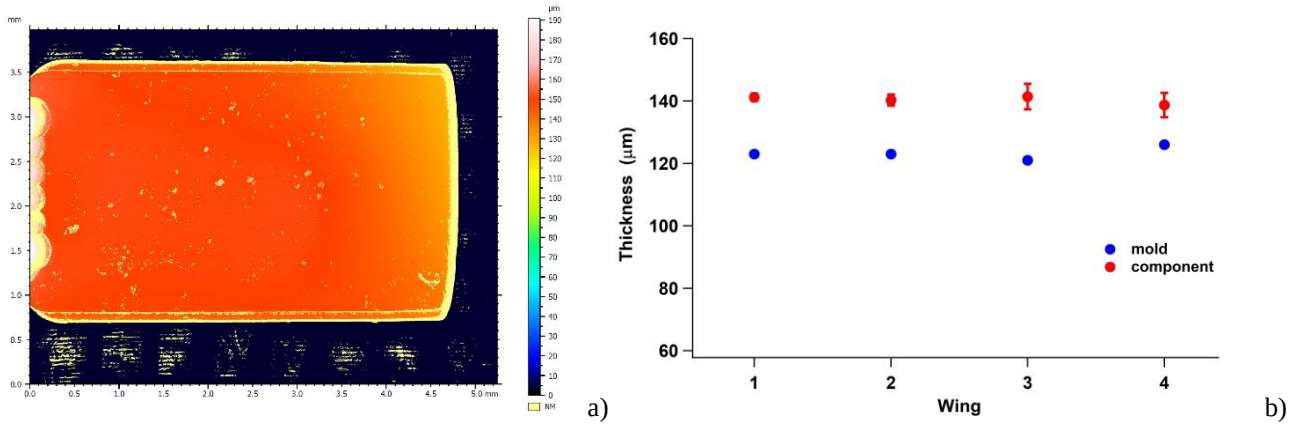

Fig. 11 a) Interferometer scan of component 1 and b) thickness results

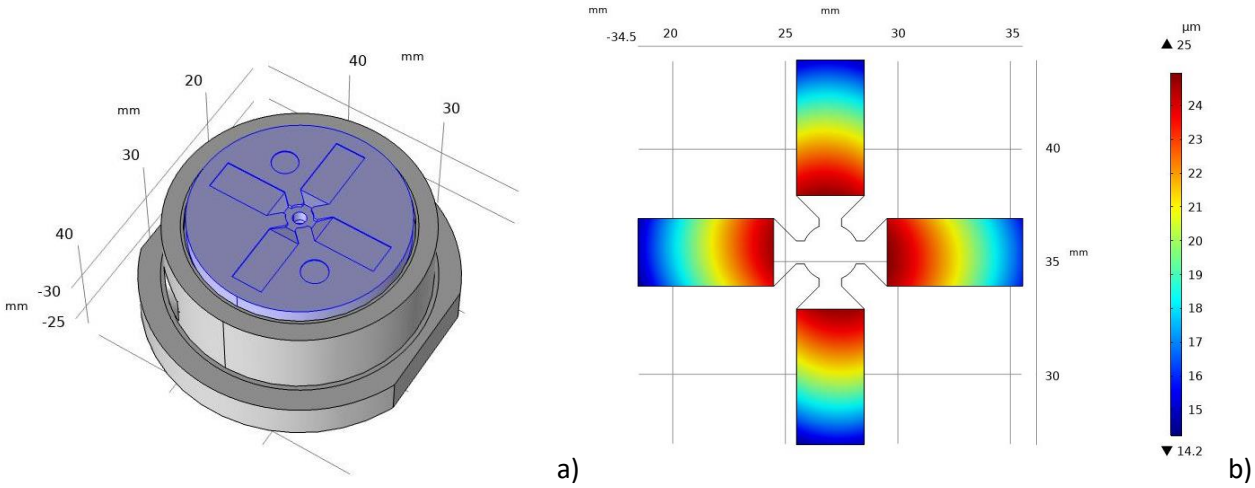

Fig. 12 a) Model of the assembled mold (steel milled tool in blue and resin support in grey) and b) displacement magnitude in z direction of the cavities

4.4 Parts roughness evaluation

For each part, six equidistant surface profiles on the length and five on the width (Fig. 13) were acquired and for each profile the roughness was evaluated after a waviness correction (Table 5). Figure 14 reports the roughness values compared between parts and wings according to the parallel (a) and orthogonal (b) flow directions. As reported in Fig. 2b, the mold wings 1 and 3 were machined parallel to the flow direction while 2 and 4 in perpendicular. Generally, pattern transfer to the parts is accurate and the parts roughness is comparable with wings value; low variability appears except for the wing having high roughness where emerges a higher dispersion of the values. This is mainly due to some discontinuities observable on the wing surface produced when the tool penetrates the part after every direction change, which is a setting imposed by the CAM software.

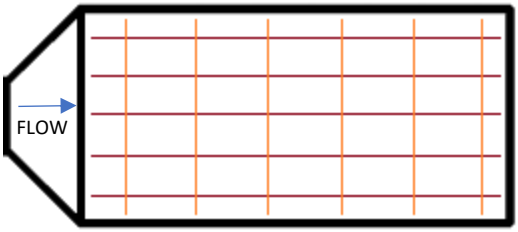

Fig. 13 Acquired roughness profiles on each component.

Table 5 Components roughness results

Ra (μm)	1	2	3	4
Profiles parallel to flow direction	0.09	0.17	0.13	0.99
	0.11	0.15	0.12	0.46
	0.13	0.15	0.14	0.12
	0.11	0.11	0.16	0.53
	0.14	0.20	0.11	1.05
Mean value	**0.12**	**0.16**	**0.13**	**0.63**
Std_dev	0.02	0.03	0.02	0.39
Profiles orthogonal to flow direction	0.07	0.07	0.81	0.18
	0.09	0.10	0.24	0.24
	0.08	0.11	0.12	0.22
	0.09	0.12	0.13	0.13
	0.08	0.11	0.12	0.09
	0.11	0.10	0.20	0.11
Mean value	**0.09**	**0.10**	**0.27**	**0.16**
Std_dev	0.01	0.02	0.27	0.06

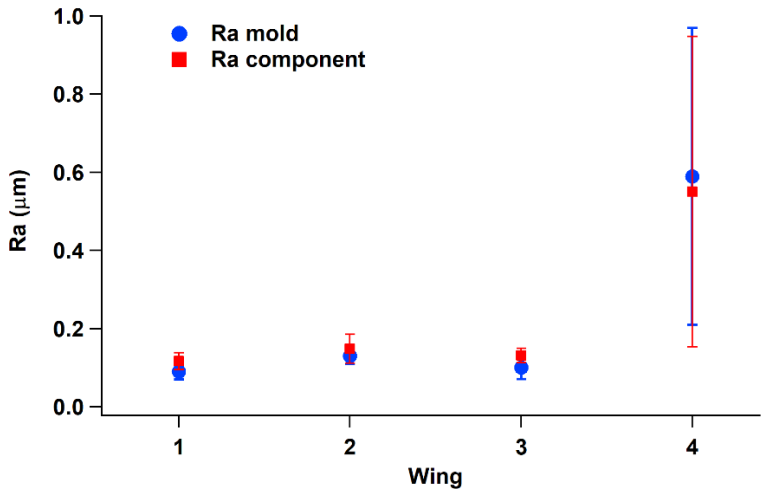

a)

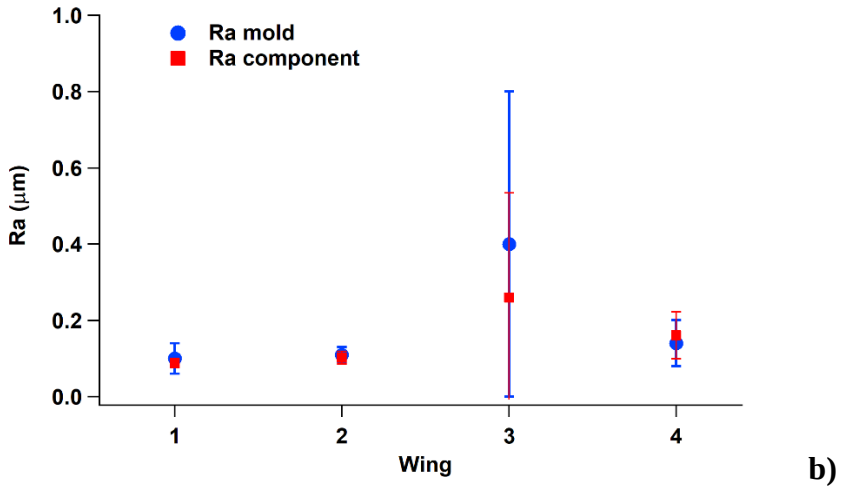

Fig. 14 Roughness values parallel (a) and orthogonal (b) to the polymer flow direction of the wings and components

4.5 Economic analysis

Beyond the quality of the molded specimen, to evaluate the feasibility of proposed integrated approach, the production time and cost were estimated and compared. The objective of this economic analysis is to highlight the advantages of the implemented process chain aiming at decreasing time and cost for injection molding tooling. The times and costs, reported in Table 6, were calculated considering times and costs regarding: pre-processing, machining, material and operator. Three process chains were compared to evaluate the best trade-off between time and costs. The three considered options are:

1. Steel mold realised by mean of two processes: turning and micro electro discharge machining (EDM) for the cavities.
2. SLA mold realised by the SLA machine using a high temperature resin.
3. Assembled mold joining the support realised by SLA and the steel disk by micro milling, presented in this research.

Through the use of synergies between manufacturing processes (option 3), it is possible to reduce the production cost of the mold of almost 74% with respect to the first option with the same manufacturing time (support and disk can be produced simultaneously).

If the mold would be realised entirely by SLA, it will request costs considerably lower than others processes but it will be suitable only for small series production being subjected rapidly to failure [33,34]. Moreover, the production time is the highest.

Table 6 Times and costs for different mold manufacturing options

OPTIONS	MATERIALS	PROCESS	TIME (h)	COST (euro)
1	Steel	turning + micro EDM	10	480
2	Hard resin	SLA	12	26

3	Steel + resin	SLA for support + Micro milling for disk	10	125

5 Conclusions

In this paper, a process chain has been proposed for polymeric part manufacturing. Stereolithography and micro-milling were applied to realise an interchangeable mold insert constituted by a support and a disk containing thin cavities, and finally the injection molding process to obtain the entire parts. This mold concept with removable insert has been adopted as a key enabling technology for answering the demand of a rapid development of components. In fact, in this way, different geometries can be obtained only replacing the milled tool minimising mold manufacturing cost and increasing versatility.

The validation was carried out through systematic analysis including feature fidelity control and mold and parts topography. The results show that the dimensional accuracy of the injected parts is good considering that thin cavities are a critical feature to be molded. No failure occurs to the resin support during screening and process settings. The research has demonstrated the possibility to reduce manufacturing cost of almost 70%. The proposed method has the potential to be applied for rapid manufacturing of other micro components.

Acknowledgements

Eng. Vito Basile is kindly acknowledged for helpful contribution in SLA support building and economic evaluation.

References

[1] Cheng, K., and Huo, D., 2013, *Micro-Cutting: Fundamentals and Applications* DOI: 10.1002/9781118536605.

[2] Azaman, M. D., Sapuan, S. M., Sulaiman, S., Zainudin, E. S., and Khalina, A., 2013, "Shrinkages and Warpage in the Processability of Wood-Filled Polypropylene Composite Thin-Walled Parts Formed by Injection Molding," Mater. Des., **52**, pp. 1018–1026 DOI: 10.1016/j.matdes.2013.06.047.

[3] Kim, D. H., and Song, Y. S., 2019, "Micro-Injection Molding Using a Polymer Coated Mold," Microsyst. Technol., **25**(10), pp. 4011–4017 DOI: 10.1007/s00542-019-04320-7.

[4] Liao, Q., Zhou, C., Lu, Y., Wu, X., Chen, F., and Lou, Y., 2019, "Efficient and Precise Micro-Injection Molding of Micro-Structured Polymer Parts Using Micro-Machined Mold Core by WEDM," Polymers (Basel)., **11**(10) DOI: 10.3390/polym11101591.

[5] Surace, R., Bellantone, V., Trotta, G., and Fassi, I., 2017, "Replicating Capability

Investigation of Micro Features in Injection Moulding Process," J. Manuf. Process., **28**, pp. 351–361 DOI: 10.1016/j.jmapro.2017.07.004.

[6] Bellantone, V., Surace, R., Trotta, G., and Fassi, I., 2013, "Replication Capability of Micro Injection Moulding Process for Polymeric Parts Manufacturing," Int. J. Adv. Manuf. Technol., **67**(5–8), pp. 1407–1421 DOI: 10.1007/s00170-012-4577-2.

[7] Lu, Y., Chen, F., Wu, X., Zhou, C., Lou, Y., and Li, L., 2019, "Fabrication of Micro-Structured Polymer by Micro Injection Molding Based on Precise Micro-Ground Mold Core," Micromachines, **10**(4) DOI: 10.3390/mi10040253.

[8] Lu, Y., Chen, F., Wu, X., Zhou, C., Zhao, H., Li, L., and Tang, Y., 2019, "Precise WEDM of Micro-Textured Mould for Micro-Injection Molding of Hydrophobic Polymer Surface," Mater. Manuf. Process., **34**(12), pp. 1342–1351 DOI: 10.1080/10426914.2019.1660784.

[9] Rötting, O., Röpke, W., Becker, H., and Gärtner, C., 2002, "Polymer Microfabrication Technologies," Microsyst. Technol., **8**(1), pp. 32–36 DOI: 10.1007/s00542-002-0106-9.

[10] Attia, U. M., Marson, S., and Alcock, J. R., 2009, "Micro-Injection Moulding of Polymer Microfluidic Devices," Microfluid. Nanofluidics, **7**(1), pp. 1–28 DOI: 10.1007/s10404-009-0421-x.

[11] Regi, F., Basso, A., Kain, M., Loaldi, D., Li, D., Zhang, Y., and Tosello, G., 2020, "Influences of Micro-Ridges Orientation and Position on the Replication of Micro-Structured Surfaces by Injection Molding," *AIP Conference Proceedings*, American Institute of Physics Inc. DOI: 10.1063/1.5142928.

[12] Sorgato, M., Zanini, F., Masato, D., and Lucchetta, G., 2020, "Submicron Laser-Textured Vents for Self-Cleaning Injection Molds," J. Appl. Polym. Sci., **137**(42) DOI: 10.1002/app.49280.

[13] Zhang, N., Liu, J., Zhang, H., Kent, N. J., Diamond, D., and Gilchrist, M. D., 2019, "3D Printing of Metallic Microstructured Mould Using Selective Laser Melting for Injection Moulding of Plastic Microfluidic Devices," Micromachines, **10**(9) DOI: 10.3390/mi10090595.

[14] León-Cabezas, M. A., Martínez-García, A., and Varela-Gandía, F. J., 2017, "Innovative Advances in Additive Manufactured Moulds for Short Plastic Injection Series," Procedia Manuf., **13**, pp. 732–737 DOI: 10.1016/j.promfg.2017.09.124.

[15] Tosello, G., Fillon, B., Azcarate, S., Schoth, A., Mattsson, L., Griffiths, C., Staemmler, L., and Bolt, P. J., 2007, "Hybrid Tooling Technologies and Standardization for the Manufacturing of Inserts for Micro Injection Molding," Annu. Tech. Conf. - ANTEC, Conf. Proc., **5**, pp. 2946–2950.

[16] Basinger, K., Webster, C., Keough, C., Wysk, R., and Harrysson, O., 2020, "Advanced Manufacturing Using Linked Processes: Hybrid Manufacturing," *Mass Production Processes*, IntechOpen DOI: 10.5772/intechopen.88560.

[17] Rahmati, S., and Dickens, P., 2007, "Rapid Tooling Analysis of Stereolithography Injection Mould Tooling," Int. J. Mach. Tools Manuf., **47**(5 SPEC. ISS.), pp. 740–747 DOI: 10.1016/j.ijmachtools.2006.09.022.

[18] Popov, K. B., Dimov, S. S., Pham, D. T., Minev, R. M., Rosochowski, A., and Olejnik, L., 2006, "Micromilling: Material Microstructure Effects," Proc. Inst. Mech. Eng. Part B J. Eng. Manuf., **220**(11), pp. 1807–1813 DOI: 10.1243/09544054JEM683.

[19] Bissacco, G., Hansen, H. N., and De Chiffre, L., 2005, "Micromilling of Hardened Tool Steel for Mould Making Applications," J. Mater. Process. Technol., **167**(2–3), pp. 201–207 DOI: 10.1016/j.jmatprotec.2005.05.029.

[20] Attanasio, A., 2017, "Tool Run-out Measurement in Micro Milling," Micromachines, **8**(7) DOI: 10.3390/mi8070221.

[21] Yuan, Y., Jing, X., Ehmann, K. F., and Zhang, D., 2018, "Surface Roughness Modeling in Micro End-Milling," Int. J. Adv. Manuf. Technol., **95**(5–8), pp. 1655–1664 DOI: 10.1007/s00170-017-1278-x.

[22] Jing, X., Li, H., Wang, J., Yuan, Y., Zhang, D., Kwok, N., and Nguyen, T., 2017, "An Investigation of Surface Roughness in Micro-End-Milling of Metals," Aust. J. Mech. Eng., **15**(3), pp. 166–174 DOI: 10.1080/14484846.2016.1211472.

[23] Zhang, X., Yu, T., and Zhao, J., 2020, "Surface Generation Modeling of Micro Milling Process with Stochastic Tool Wear," Precis. Eng., **61**, pp. 170–181 DOI: 10.1016/j.precisioneng.2019.10.015.

[24] Sun, Z., and To, S., 2018, "Effect of Machining Parameters and Toolwear on Surface Uniformity in Micro-Milling," Micromachines, **9**(6) DOI: 10.3390/mi9060268.

[25] Wang, W., Kweon, S. H., and Yang, S. H., 2005, "A Study on Roughness of the Micro-End-Milled Surface Produced by a Miniatured Machine Tool," J. Mater. Process. Technol., **162**–**163**(SPEC. ISS.), pp. 702–708 DOI: 10.1016/j.jmatprotec.2005.02.141.

[26] Sodemann, A., Li, M., Mayor, R., and Forest, C. R., 2009, "Micromilling of Molds for Microfluidic Blood Diagnostic Devices," Proc. 24th Annu. Meet. Am. Soc. Precis. Eng. ASPE 2009.

[27] Vázquez, E., Amaro, A., Ciurana, J., and Rodríguez, C. A., 2015, "Process Planning Considerations for Micromilling of Mould Cavities Used in Ultrasonic Moulding Technology," Precis. Eng., **39**, pp. 252–260 DOI: 10.1016/j.precisioneng.2014.07.001.

[28] Chen, P. C., Chen, Y. C., Pan, C. W., and Li, K. M., 2015, “Parameter Optimization of Micromilling Brass Mold Inserts for Microchannels with Taguchi Method,” Int. J. Precis. Eng. Manuf., **16**(4), pp. 647–651 DOI: 10.1007/s12541-015-0086-1.

[29] Davoudinejad, A., Li, D., Zhang, Y., and Tosello, G., 2020, “Effect of Progressive Tool Wear on the Functional Performance of Micro Milling Process of Injection Molding Tool,” Procedia CIRP, **87**, pp. 159–163 DOI: 10.1016/j.procir.2020.02.031.

[30] Surace, R., Sorgato, M., Bellantone, V., Modica, F., Lucchetta, G., and Fassi, I., 2019, “Effect of Cavity Surface Roughness and Wettability on the Filling Flow in Micro Injection Molding,” J. Manuf. Process., **43**(November 2018), pp. 105–111 DOI: 10.1016/j.jmapro.2019.04.032.

[31] Bellantone, V., Surace, R., Modica, F., and Fassi, I., 2018, “Evaluation of Mold Roughness Influence on Injected Thin Micro-Cavities,” Int. J. Adv. Manuf. Technol., **94**(9–12), pp. 4565–4575 DOI: 10.1007/s00170-017-1178-0.

[32] Bártolo, P. J., 2011, “Stereolithography - Materials, Processes and Applications,” Springer, p. 340.

[33] Valori, M., Surace, R., Basile, V., Luzi, L., Vertechy, R., and Fassi, I., 2020, “Rapid Fabrication of POM Flexure Hinges via a Combined Injection Molding and Stereolithography Approach,” Proc. ASME Des. Eng. Tech. Conf., **1** DOI: 10.1115/DETC2020-22476.

[34] Bagalkot, A., Pons, D., Symons, D., and Clucas, D., 2019, “Categorization of Failures in Polymer Rapid Tools Used for Injection Molding,” Processes, **7**(1) DOI: 10.3390/pr7010017.